Brookes, P., N & Lawley, P. D. (1961) *J. Chem. Soc.*, 3923.
Collins, C. J., & Guild, W. R. (1968) *Biochim. Biophys. Acta 157*, 107–113.
Dubelman, S., & Shapiro, R. (1977) *Nucleic Acids Res. 4*, 1815–1827
Essigman, J. M., Croy, R. G., Nadzan, A. M., Busby, W. F., Jr., Reinhold, V. N., Buchi, G., & Wogan, G. N. (1977) *Proc. Natl. Acad. Sci. U.S.A. 74*, 1870–1874.
Feldman, M. Ya. (1967) *Biochim. Biophys. Acta 149*, 20–34.
Feldman, M. Ya. (1973) *Prog. Nucleic Acid Res. Mol. Biol. 13*, 1–47.
Fraenkel-Conrat, H. (1954) *Biochim. Biophys. Acta 15*, 307–309.
Freifelder, D., & Davison, P. F. (1963) *Biophys. J. 3*, 49–63.
Fritz, H. J., Belagaje, R., Brown, E. L., Fritz, R. N., Jones, R. A., Lees, R. G., & Khorana, H. J. (1978) *Biochemistry 17*, 1257–1267.
Hartwick, R. A., & Brown, P. R. (1976) *J. Chromatogr. 126*, 679–691.
Jeffrey, A. M., Blobstein, S. H., Weinstein, I. B., & Harvey, R. G. (1976) *Anal. Biochem. 73*, 378–385.
Karger, B. L., & Giesen, R. W. (1978) *Anal. Chem. 50*, 1048A–1059A.
McGhee, J. D., & Von Hippel, P. H. (1977) *Biochemistry 16*, 3276.
Nature (London) (1979) *281*, 625.
Shapiro, R., Dubelman, S., Feinberg, A. M., Crain, P. F., & McCloskey, J. A. (1977) *J. Am. Chem. Soc. 99*, 302–303.
Singer, B. (1972) *Biochemistry 11*, 3939.
Singer, B. (1975) in *CRC Handbook of Biochemistry and Molecular Biology* (Tanuan, G. D., Ed.) 3rd ed., Vol. I, p 409, CRC Press, Cleveland, OH.
Van Der Eb, A. J., Van Kesteren, L. W., & Van Bruggen, E. F. (1969) *Biochim. Biophys. Acta 182*, 530–541.

Fluorescence of Terbium Ion–Nucleic Acid Complexes: A Sensitive Specific Probe for Unpaired Residues in Nucleic Acids†

Michael D. Topal and Jacques R. Fresco*

ABSTRACT: The interaction of the lanthanide cation Tb^{3+} with the phosphate moieties of non-hydrogen-bonded residues of nucleic acids has been shown to result in substantial enhancement of the fluorescence of this cation. The excitation spectrum for this fluorescence is characteristic of the base moiety of the residue to which the Tb^{3+} is bound, while the emission spectrum is characteristic of the cation itself. The intensity of the fluorescence enhancement, however, is dependent upon the base of the ligand moiety, with G inducing the strongest enhancement, C and T rather less, and A very little. Base-paired residues of nucleic acids induce *no* such fluorescence enhancement, even though the cation is more tightly bound to double helical regions than to residues in single strands. The enhancement of Tb^{3+} fluorescence upon binding to non-hydrogen-bonded residues therefore provides a highly specific conformational probe for such residues. This probe has been exploited successfully for the purpose of analyzing the kinetics of reassociation of DNAs (C_0t analysis) and as a specific stain for single-strand DNA bands on polyacrylamide gels.

The rare-earth lanthanide Tb^{3+} (terbium ion) exhibits a low level of intrinsic fluorescence that is enhanced many-fold upon interaction with GMP (Formosa, 1973). This behavior is consistent with findings that there is general enhancement of the fluorescence of rare-earth cations by energy transfer from excited ligands chelating the ion (Weissman, 1942, 1950; Yuster & Weissman, 1949). The site of Tb^{3+} binding to nucleic acid monomers appears to be their negatively charged phosphate moiety, as has been shown for other lanthanide ions (Barry et al., 1971), which is to be expected in view of the generally observed strong affinity of trivalent cations for the nucleic acid backbone [e.g., Karpel et al. (1975, 1980)]. We have therefore explored the possibility that the concentration of charge in the nucleic acid backbone might result in greater enhancement of the fluorescent emission of Tb^{3+}. Since the nature of the base and its involvement in polynucleotide secondary structure should influence the transfer of energy to the bound Tb^{3+}, we also examined whether there is any secondary structural and/or base specificity to the enhanced Tb^{3+} fluorescence. In fact, all three effects were observed: Tb^{3+} bound to unpaired residues in nucleic acid chains exhibits much greater fluorescence than when bound to free nucleotides in solution; the amount of fluorescence enhancement depends on the identity of the residue; Tb^{3+} bound to *base-paired* residues shows no fluorescence enhancement. These properties enable the use of Tb^{3+} as a sensitive and specific stain for unpaired nucleic acid residues in solution and on gels. In this respect, the fluorescent behavior of Tb^{3+} on binding to nucleic acids complements that of ethidium bromide, which exhibits strong fluorescence on binding to double-stranded DNA but only weak fluorescence on binding to single strands (LePecq & Paoletti, 1967). A preliminary report of this work has been made (Topal & Fresco, 1979).

Materials and Methods

Materials. $TbCl_3$ (D. F. Goldsmith Chemical and Metal Corp.) was used without further purification. Cacodylic acid was recrystallized from hot 50% ethanol. Guanosine and nucleotides (Sigma Chemical Co.) were used without further purification.

† From the Department of Biochemical Sciences, Princeton University, Princeton, New Jersey 08544 (J.R.F.), and the Department of Pathology and the Cancer Research Center, University of North Carolina Medical School, Chapel Hill, North Carolina 27514 (M.D.T.). *Received February 14, 1980.* This work was supported by a National Cancer Institute Postdoctoral Fellowship to M.D.T. at Princeton University, Grant IN-15-S from the American Cancer Society and Grant P30 CA 16086 from the National Institutes of Health to M.D.T. at the University of North Carolina, and Grant GM 07654 from the National Institutes of Health and Grant GB 35595 from the National Science Foundation to J.R.F. at Princeton University. This is paper 17 in a series entitled "Polynucleotides", of which the previous paper is Karpel et al. (1980).

0006-2960/80/0419-5531$01.00/0

Poly(ribonucleotides) were synthesized from the appropriate nucleoside diphosphates by using polynucleotide phosphorylase (Grunberg-Manago et al., 1956). The polymers were freed of protein by repeated phenol extraction, dialyzed vs. 1 M NaCl + 0.1 M EDTA and then against four changes of doubly distilled water, and isolated as the sodium salt by lyophilization. Base composition of poly(C_{75},G_{25}) copolymer was determined by multicomponent spectral analysis (Guschlbauer et al., 1965) of neutralized alkaline hydrolysates (0.3 N KOH at 38 °C for 36 h, followed by 2 h at 25 °C in 0.2 N HCl, and then neutralized to pH 7, 0.01 M cacodylate). The library spectra for these analyses were those for 2′,3′-CMP and 2′,3′-GMP.

Deoxyhomopolymers (Miles Laboratories) were dialyzed as were the poly(ribonucleotides). All DNA samples, calf thymus DNA (Miles Laboratories), T-5 and T-7 bacteriophage DNAs (gifts from B. Alberts), chick embryo red cell total DNA (gift from H. Weintraub), and *Hae*III-digested PM2 DNA (gift from B. Alberts), were first exhaustively dialyzed vs. 1 M NaCl + 0.1 M EDTA to remove any contaminants, which were sometimes present, that enhance Tb^{3+} fluorescence. Finally, they were equilibrated by dialysis with 0.01 M cacodylate (pH 7), in which they could be stored in the native conformation.

Fluorescence Measurements. Fluorescence emission and excitation spectra were measured with Perkin-Elmer spectrofluorometers, Model MPF 4 at Princeton University and Model MPF 2A at the University of North Carolina. In both instruments the light source was a high-pressure xenon lamp. Both instruments were calibrated before each use with a solution of 10^{-8} M quinine sulfate in 0.1 M H_2SO_4. So that the data obtained in both were fully comparable, spectral data were also normalized for other small instrument differences. A 390-nm filter was employed to eliminate scattered light. This filter eliminated a large emission peak centered near 360 nm, which interfered with the major Tb^{3+} emission peak at 545 nm. Both instruments were free of drift over a 4-h measuring period and relatively noise free at the sensitivities used. Excitation and emission slits of 20 and 10 nm, respectively, gave adequate resolution and good sensitivity.

Tb^{3+} Fluorescence Enhancement Experiments. A fresh stock solution of Tb^{3+} in 0.01 M cacodylate (pH 7) was prepared for each experiment, and aliquots were added to nucleic acid solutions *just* prior to measurement. This was especially important with RNA samples since lanthanides slowly catalyze hydrolysis of their internucleotide bonds (Eichorn & Butzow, 1965). In all experiments, nucleotide residue concentration was 10^{-4} M, the same level generally used for ultraviolet absorbance measurements of nucleic acids. The solutions were then titrated with Tb^{3+} to determine the fluorescence enhancement over that of Tb^{3+} alone in the same buffer at the same concentration. Thus, fluorescence values are reported after subtracting the unenhanced fluorescence of the Tb^{3+} present, were it free. By titrating with Tb^{3+} at fixed nucleic acid concentration, rather than the reverse, as was done in other recent studies (Yonuschot & Mushrash, 1975; Ringer et al., 1978), it was possible to determine the optimal levels of Tb^{3+} required to give readily measurable fluorescence at a convenient low nucleic acid concentration and also to directly compare, on a molar basis, the fluorescence enhancement of different nucleic acid samples.

Results

Fluorescence of Tb^{3+}–Nucleotide Complexes. Terbium ion has a fluorescence (emission) spectrum consisting of two peaks, a smaller one centered at about 490 nm and a larger peak with λ_{max} at 545 nm (Figure 1). The excitation (absorption)

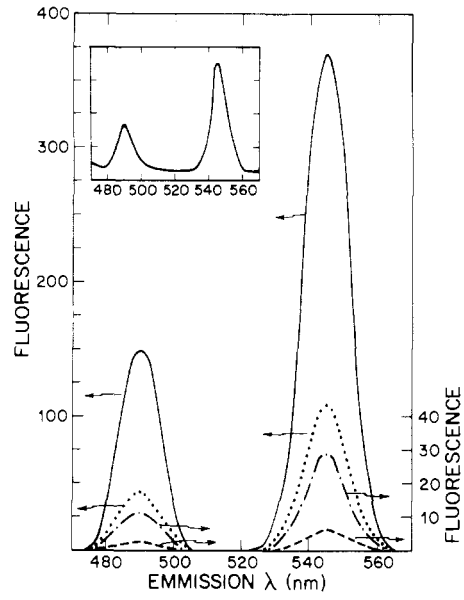

FIGURE 1: Emission spectra of free Tb^{3+} (1.5×10^{-4} M) (---), Tb^{3+} (1.5×10^{-4} M) complexed to dGMP (–·–), poly(dG) (···), and denatured calf thymus DNA (—); residue concentrations were 1×10^{-4} M in all cases. Solvent: 0.01 M cacodylate, pH 7.8. Spectra were measured at 25 °C except for Tb^{3+}-denatured DNA, which was determined at 4 °C. Spectra were not corrected for the inherent fluorescence of Tb^{3+} were it free in solution, but were corrected for base line variations. The uncorrected raw spectrum for Tb^{3+}-denatured calf thymus DNA is shown in the inset.

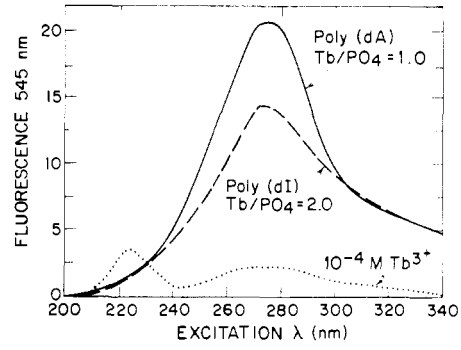

FIGURE 2: Fluorescence excitation spectra of free Tb^{3+} (10^{-4} M) and of Tb^{3+} in the presence of poly(dA) (10^{-4} M) and poly(dI) (10^{-4} M). Solvent: 0.01 M cacodylate, pH 7.8.

spectrum of Tb^{3+} monitored from the fluorescence at 545 nm (Figure 2) consists of a peak with λ_{max} at 222 nm and a broad band centered at about 275 nm. The intensity of the fluorescence of free Tb^{3+} when excited at absorption λ_{max} is very small (Figures 1 and 2), while the standard (unmodified) nucleic acid residues, either as monomers or when in DNA or RNA polymers, display essentially no fluorescence at 25 °C. However, complex formation between Tb^{3+} and certain ribo- and deoxynucleoside phosphates, particularly those of guanine, results in substantial enhancement of the fluorescence above that of Tb^{3+} alone (Figure 1). The spectrum of this fluorescence retains λ_{max} at 545 nm, regardless of the base in the nucleotide, though the relative intensity of the fluorescence does vary with the base (Figure 1 and Table I, left side). On the other hand, λ_{max} of the excitation spectrum (Table I and Figures 2–4) does vary somewhat with the base. This is consistent with the idea that the observed fluorescence enhancement is due to long-range energy transfer from particular electronic transitions in each base to the same electronic transition in Tb^{3+} (characterized by the 275-nm band of free Tb^{3+}). Nevertheless, since uncharged guanosine and singly

Table I: Fluorescence of Tb^{3+}–Nucleic Acid Complexes[a]

monomer (10^{-4} M/L)	excitation λ_{max} (nm)	fluorescence emission,[b] λ_{545} $[Tb^{3+}]$ = 1.5×10^{-4} M	fluorescence emission,[b] λ_{545} $[Tb^{3+}]$ = 5×10^{-4} M	polymer[c] (10^{-4} M residues/L)	excitation λ_{max} (nm)	fluorescence emission,[b] λ_{545} $[Tb^{3+}]$ = 1.5×10^{-4} M
dAMP	-	0	0	poly(dA)	276	18
AMP	284	1	5	poly(A)	276	24
dCMP	-	0	0	poly(dC)	283	53
CMP	285	4	7	poly(C)	283	210
dTMP	265	2	2	poly(dT)	280	113
UMP	265	14	15			
IMP	-	0	0	oligo(I_4)	275	18
				poly(dI)	274	13
G	-	0	0			
3′,5′-cGMP	-	0	0			
dGMP	287	23	80	poly(dG)	287	103
GMP	287	13	35	poly(G)	287	224 (391)[d]
GDP	287	73	85			
GTP	286	53	116			
				nat. T-7 DNA	-	0
				den. T-7 DNA	287	380
				nat. T-5 DNA	-	0
				den. T-5 DNA	287	350
				nat. CT DNA	-	0
				den. CT DNA	287	365

[a] Solvent is 0.01 M cacodylate, pH 7. [b] Value after subtracting the inherent fluorescence of the Tb^{3+} present, were it all free; i.e., $I_1 - I_0$. To convert these values to $(I_1 - I_0)/I_0$, the reader is referred to the dotted spectrum in Figure 2, which presents the I_0 values for $[Tb^{3+}] = 1.0 \times 10^{-4}$ M. Fluorescence emission for Tb^{3+} is linear with concentration to 5×10^{-4} M. [c] nat. = native; den. = denatured; CT = calf thymus. [d] Value in the presence of 1 M urea.

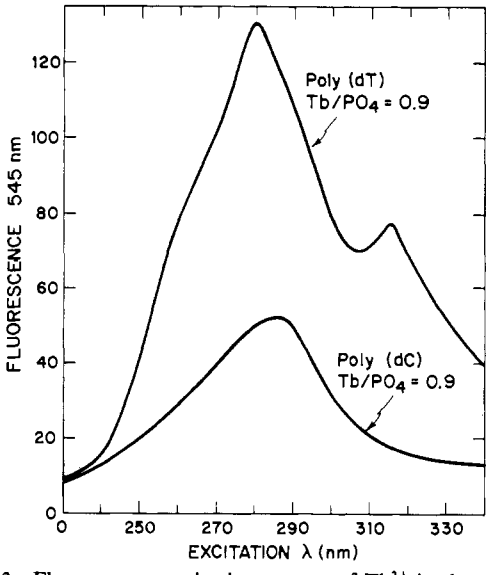

FIGURE 3: Fluorescence excitation spectra of Tb^{3+} in the presence of poly(dT) (10^{-4} M) and poly(dC) (10^{-4} M). Solvent: 0.01 M cacodylate, pH 7.8.

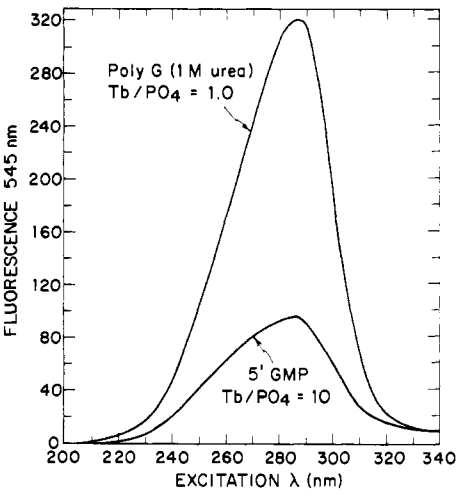

FIGURE 4: Fluorescence excitation spectra of Tb^{3+} in the presence of 5′-GMP (10^{-4} M) and poly(G) (10^{-4} M). Solvent: 0.01 M cacodylate, pH 7.8, with 1 M urea for the poly(G) only.

charged cGMP exhibit no fluorescence enhancement whereas the enhancement progresses in direct proportion to the number of additional negative charges on the guanine nucleotide (Table I), chelation of the Tb^{3+} must occur by direct Coulombic interaction with the phosphate center of negative charge and not with the bases themselves.

Fluorescence of Tb^{3+}–Homopolynucleotide Complexes. As was found with Tb^{3+}–nucleotide complexes, Tb^{3+}–homopolynucleotide complexes exhibit essentially the same emission spectrum as free Tb^{3+} (Figure 1), except that now the relative intensity of fluorescence is greatly enhanced, particularly for poly(C), poly(dC), poly(dT), poly(dG), and poly(G) (Table I, right side). Also following a trend seen with Tb^{3+}–monomer complexes, polymers with ribose in the backbone enhance Tb^{3+} fluorescence much more than those with deoxyribose. The excitation spectra for several homopoly(deoxynucleotides) are shown in Figures 2 and 3, while those for 5′-GMP and poly(G) in 1 M urea are presented in Figure 4. In general, these excitation spectra resemble those of the Tb^{3+}–nucleotide complexes, though, as noted above, intensities are very much greater. However, the Tb^{3+}–poly(dT) complex does not conform to this pattern, as its excitation λ_{max} is located at 280 nm, which is 15 nm to the red of its location for Tb^{3+}–TMP. The excitation spectrum of Tb^{3+}–TMP consists of three partially resolved peaks (not shown), whereas that of Tb^{3+}–poly(dT) contains a shoulder on either side of the peak (Figure 3). It is one of the minor peaks of Tb^{3+}–TMP that seems to be preferentially enhanced in Tb^{3+}–poly(dT).

Table I shows that there is nearly a doubling of the fluorescence enhancement by poly(G) when 1 M urea is present. Poly(G) strands have a strong tendency to form four-stranded helixes (Fresco & Massoulie, 1963; Zimmerman et al., 1975) involving tetrads of hydrogen-bonded guanosine residues, and 1 M urea is a mild denaturant of hydrogen-

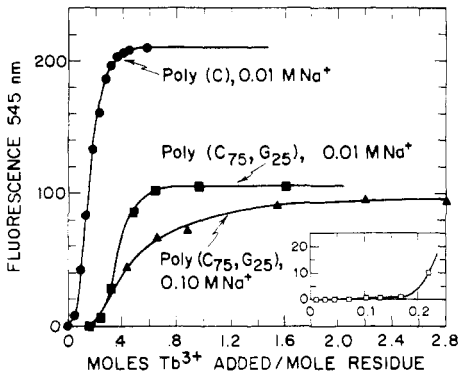

FIGURE 5: Titration of poly(C) (10^{-4} M) and poly(C_{75},G_{25}) (10^{-4} M) with Tb^{3+}, monitored from the fluorescence emission at 545 nm. Solvent: 0.01 M cacodylate, pH 7.8, and the indicated [Na^+].

bonded bases. Since urea alone had no effect on the intrinsic fluorescence intensity of free Tb^{3+} and only a very small effect on the fluorescence of Tb^{3+}–GMP, its fluorescence enhancing effect can be associated with its ability to denature the poly(G) hydrogen-bonded helical structure. Hence, it would appear that the occurrence of the G residues in a helically stacked hydrogen-bonded conformation suppresses the fluorescence yield of Tb^{3+}–poly(G). It should be noted also that the multistranded poly(G) helical structure is difficult to form perfectly without annealing, so that an even greater level of suppression would be expected if all the poly(G) residues were involved in hydrogen-bonded base–base interactions (see below). This implies that in the absence of urea, it is the non-hydrogen-bonded G residues of poly(G) that account for the enhancement of the Tb^{3+} fluorescence. This possibility is further explored below with polynucleotides that can be readily induced to form base-paired double helixes quantitatively.

Stoichiometry and Strength of Binding of Tb^{3+} to Polynucleotides. These properties were determined by titrating poly(C) with Tb^{3+}, using the fluorescence enhancement at 545 nm to monitor the interaction. Poly(C) was selected for this quantitative study because it is single stranded in 0.01 M cacodylate (pH 7) and induces substantial fluorescence on binding the cation. Moreover, it is reasonable to assume that all the binding sites on a homopolymer are equivalent and that energy transfer from all its bases is the same, so that fluorescence enhancement should be linearly related to stoichiometry. We can, therefore, define K, the equilibrium association constant for nucleoside residue binding to Tb^{3+} binding sites, as

$$K = \frac{[\text{bound residues}]}{[\text{free residues}](n[Tb^{3+}] - [\text{bound residues}])}$$

where [bound residues] and [free residues] are the concentrations of nucleic acid residues bound and unbound to Tb^{3+}, respectively, n is the number of binding sites per Tb^{3+}, and [Tb^{3+}] is the total concentration of Tb^{3+}. By rearranging, a linear equation is obtained thus:

$$\frac{[Tb^{3+}]}{[\text{bound residues}]} = \frac{1}{nK[\text{free residues}]} + \frac{1}{n}$$

Hence, a plot of [Tb^{3+}]/[bound residues] vs. 1/[free residues] should give a straight line. The reciprocal of the intercept of this line, i.e., n, then determines the number of poly(C) residues binding to one Tb^{3+}, and the intercept divided by the slope of the line, i.e., K, gives the affinity of one residue for a Tb^{3+}.

Figure 5 shows how the fluorescence increases as poly(C) is titrated with Tb^{3+}. Except for a very small lag at very low [Tb^{3+}], the fluorescence dependence on [Tb^{3+}] is hyperbolic.

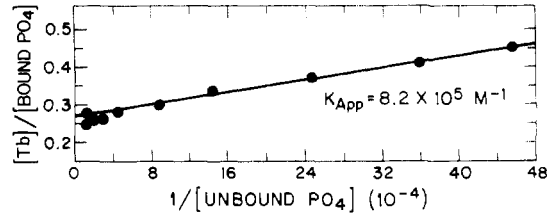

FIGURE 6: Plot of [Tb]/[bound PO_4] vs. 1/[unbound PO_4] (see text) for poly(C) residue binding to Tb^{3+}. Data are taken from Figure 5.

The reason for this small lag is not immediately obvious; it could be due to a small amount of cooperativity in Tb^{3+} binding, or to a low level of damaged residues in the poly(C), or to a low level of hemiprotonated poly(C·C^+), which can occur at pH 7 in 0.01 M Na^+ at 25 °C (Guschlbauer, 1967). In any case, this lag is of no consequence for the analysis, since Figure 6 shows that the data conform well with the expected linear plot. From the intercept and slope, it is determined that 1 Tb^{3+} binds to 3.7 polynucleotide residues with an affinity of 8.2×10^5 M^{-1}. A binding constant of this magnitude is not unreasonable for a trivalent cation binding to the negatively charged phosphates in the absence of stereochemically well-defined binding sites as would result from either the grooves in double-helical secondary structure (Karpel et al., 1980) or well formed pockets as in the tertiary structure of tRNA (Karpel et al., 1975). What is perhaps unexpected in view of the single negative charge associated with each phosphate of the polynucleotide backbone is the finding that it takes 3.7 rather than 3 nucleic acid residues to bind 1 Tb^{3+}. Perhaps, the additional 0.7 residue reflects the effect of Debye–Huckel shielding by the 0.01 M Na^+ present, which reduces the effectiveness of the Coulombic attraction of the polyelectrolyte anions for the free trivalent cations and also competes weakly with the Tb^{3+} for the anionic phosphate sites. That both effects play some role is indicated by the effect of increasing Na^+ concentration on the titration of poly(C_{75},G_{25}) (see Figure 5 and below).

Lack of Tb^{3+} Fluorescence Enhancement by Base-Paired Residues. If long-range energy transfer from bases is the mechanism of the enhancement of Tb^{3+} fluorescence on binding to nucleic acid residues, the perturbation of the electronic structure of bases that accompanies hydrogen-bonded base–base interaction ought to influence the efficiency of the process. In the case of poly(G), it was found (see above) that G–G interaction on helix formation suppresses the fluorescence enhancement of Tb^{3+}. Additional experiments were performed to determine whether a lack of Tb^{3+} fluorescence enhancement is characteristic of base-paired residues.

In one experiment a random copolymer of 75% C and 25% G residues was titrated with Tb^{3+}, as was done for poly(C), but in this case in solvents containing two different Na^+ concentrations, 0.01 and 0.1 M. The 25 mol % of G residues of this random copolymer should be virtually all pairable to C residues by forming G·C helixes with looped-out C residues (Fresco et al., 1960; Fresco, 1963). Thus, 50% of the residues should be base paired, while the other half (all C residues) should be unpaired. The titration results plotted in Figure 5 show that the plateau level of fluorescence of the Tb^{3+} copolymer complex is in fact just 50% that of Tb^{3+}–poly(C) even though G residues, with their much larger fluorescence enhancement of chelated Tb^{3+}, can contribute much more to the overall fluorescence enhancement of Tb^{3+} by the entire copolymer than can the looped-out C residues. Furthermore, no fluorescence is manifest until approximately 0.17 mol of Tb^{3+} is added per mol of copolymer residues; thereafter,

fluorescence rises very sharply to the palteau level (see insert, Figure 5). Since the affinity of small multivalent cations is generally much greater for residues in the duplex than in single strands [cf. Karpel et al. (1980)], it would appear that the substantial lag in appearance of fluorescence reflects the fact that Tb^{3+} bound to base-paired residues does not exhibit enhanced fluorescence.

The effect of increasing the Na^+ concentration from 0.01 to 0.1 M on the titration of poly(C_{75},G_{25}) is also shown in Figure 5. The increase has no effect on the initial lag in fluorescence enhancement until 0.17 mol of Tb^{3+} per residue is added. Also, it has little effect on the maximum amount of fluorescence enhancement that can be attained. What is affected is the shape of the titration curve. At the higher Na^+ concentration, the increase in fluorescence is much more gradual with increasing Tb^{3+}, so that the fluorescence asymptotically approaches the maximum attained in 0.01 M Na^+. Such behavior indicates weaker binding of Tb^{3+} to the unpaired C residues of the polymer in 0.1 M Na^+ than in 0.01 M Na^+ and is consistent with Tb^{3+} binding to the phosphate moieties of the residues.

Additional titration experiments were performed with DNA from calf thymus and from phages T-5 and T-7 in their double-strand native conformation and after thermal denaturation (100 °C for 3 min, fast cooled to 0 °C to prevent annealing, and measured at 4 °C). *No* fluorescence enhancement of Tb^{3+} by the native DNA samples was detected, whereas very large fluorescence enhancement by the denatured DNA was observed (Table I).[1] The excitation spectra for all three denatured DNA–Tb^{3+} complexes were identical and indistinguishable from that observed for the poly(dG)–Tb^{3+} complex (Figure 4). However, since the excitation spectra observed in the presence of the different homopolymers are so similar, it is not possible to decide from these data alone which bases in denatured DNA contribute most of the fluorescence of its complex with Tb^{3+}. The homopolymer studies do show, however, that G residues make the main contribution, with C and T making smaller but significant contributions (Table I).

Tb^{3+} Fluorescence Enhancement as a Probe of Nucleic Acid Renaturation Kinetics. The foregoing results have shown that only unpaired residues contribute to the enhancement of Tb^{3+} fluorescence. This suggests this enhancement effect as a probe for unpaired regions of nucleic acids. It should be possible, therefore, to follow the kinetics of annealing of two complementary DNA strands, using this probe to monitor the amount of single-stranded DNA remaining with increasing time. The results of such a determination for chick embryo red cell total DNA are shown in Figure 7, superimposed on the C_0t curve measured by Weintraub & Groudine (1976) for the same annealing process. Their data were obtained by using a high concentration of unlabeled DNA to drive the annealing of a small amount of radioactively labeled DNA and S_1 nuclease digestion of single-strand DNA to measure the amount of double-helix formation with time. It can be seen that the fluorescence enhancement data fit the S_1 nuclease defined curve reasonably well. That is, the percent total hybridization agrees well and the log $C_0t_{1/2}$, which could have been anywhere from approximately −6 [for poly(U) + poly(A)] to approximately +4 for mammalian nonrepetitive DNA (Britten & Kohne, 1968), is about 2.75. The good correlation between

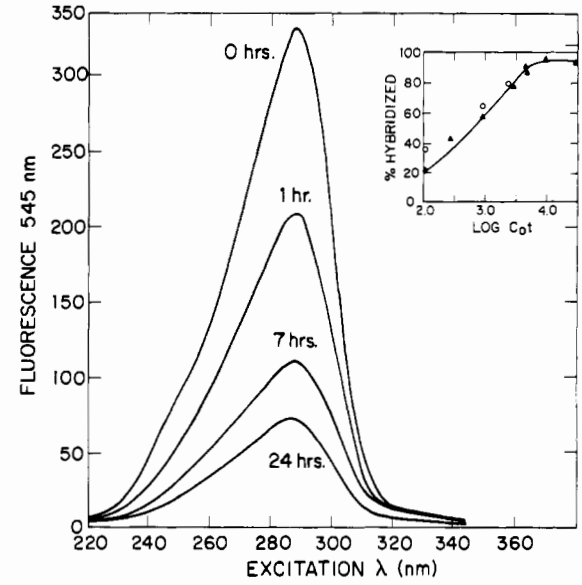

FIGURE 7: Monitoring of the kinetics of reassociation of chick red blood cell total DNA by Tb^{3+} fluorescence. Chick DNA (10 mg/mL) (Weintraub & Groudine, 1976) in 0.3 M NaCl, 50 mM Tris-HCl (pH 7.4), and 0.1% $NaDodSO_4$ was denatured at 100 °C and allowed to anneal at 65 °C in polypropylene tubes overlaid with paraffin oil. After 0, 1, 7, and 24 h of annealing, aliquots were taken, chilled to 4 °C, and diluted to a final DNA concentration of 10^{-4} M. $TbCl_3$ was added so that the $[Tb^{3+}]/[PO_4^-]$ ratio was 0.65. The excitation spectrum was measured at 4 °C by monitoring the fluorescence emission at 545 nm. The inset shows a plot of the percent hybridization calculated from these measurements (assuming that the fluorescence measured just after denaturation represents 0% hybridization and that no fluorescence is present at 100% hybridization) vs. the log of the initial concentration of DNA in moles per liter multiplied by the time in seconds at which the aliquots were taken (○). Also shown in the inset is the percent hybridization of this DNA vs. log C_0t in the region where single-copy sequences renature, as measured by Weintraub & Groudine (1976) using S_1 nuclease digestion of the unhybridized radioactive DNA (▲).

the S_1 nuclease derived C_0t curve and the Tb^{3+} fluorescence enhancement-derived data points confirms the finding that base pairing quenches the fluorescence of nucleic acid–Tb^{3+} complexes. Moreover, it suggests that the presence of Tb^{3+} does not substantially affect T_m of the DNA under the high-salt conditions of reassociation (0.3 M Na^+). For confirmation of this, the T_m of calf thymus DNA in 0.01 M cacodylate buffer (pH 7) was determined over a range of Tb^{3+} concentration from 0 to 10^{-4} M; only a 2 °C increase, from 62.3 to 64.1 °C, was observed. This experiment shows also that the Tb^{3+} probe has the advantage of not requiring radioactive nucleic acid strands for C_0t analysis.

Tb^{3+} Staining of Single-Strand DNA in Polyacrylamide Gels. The conformational specificity of enhancement of Tb^{3+} fluorescence by unpaired nucleic acid residues suggests that Tb^{3+} can be used to locate single-stranded nucleic acid bands after electrophoresis on polyacrylamide gels. Double-stranded DNA fragments produced by digestion of PM2 DNA with the restriction endonuclease *Hae*III were electrophoresed in 5% acrylamide gels. The fragments were either prepared under native conditions and run into a native gel or else denatured by heating and run into an acrylamide gel prepared with formamide to maintain the DNA in a denatured state. The results of staining these gels with either ethidium bromide, which causes only double-stranded DNA to fluoresce strongly, or $TbCl_3$ are shown in Figure 8, in the form of photographs of five slab gels presented side by side. Actually, the figure contains photographs of three different slab gels, as two of the gels were photographed twice, first after staining with ethidium

[1] This observation is in contrast to the report (Ringer et al., 1978) that native DNA shows a significant level of fluorescence in the presence of Tb^{3+}, which is enhanced on denaturation. We attribute their result to damaged or contaminated DNA.

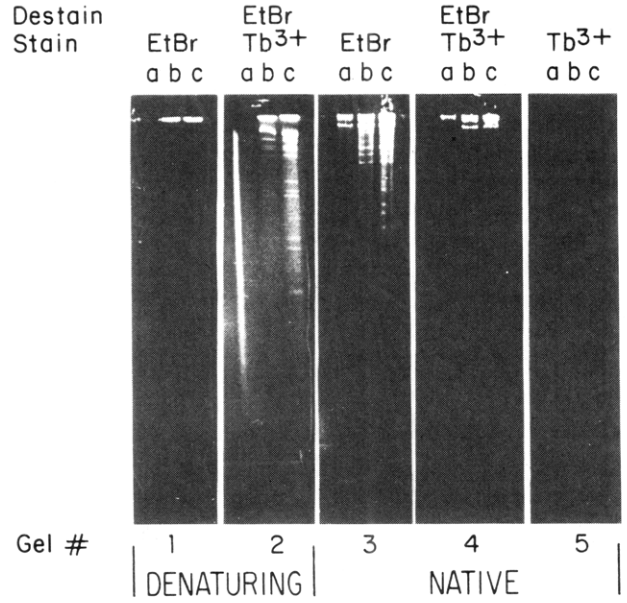

FIGURE 8: Differential staining of native and denatured PM2 DNA bands on polyacrylamide gels with ethidium bromide and terbium chloride, respectively. PM2 DNA digested with *Hae*III was electrophoresed in 5% acrylamide gels. The fragments were either denatured by heating to 100 °C for 3 min, quick cooled to 4 °C, and electrophoresed into 5% acrylamide gels prepared with formamide to maintain the DNA in the denatured state (gels 1 and 2) or kept native and electrophoresed into native 5% acrylamide gels (gels 3–5). Each series of three slots (a, b, and c) contained 0.5, 2.5, and 6.0 μg of *Hae*III-digested PM2 DNA, respectively. The formamide gel containing denatured PM2 DNA bands was stained with ethidium bromide by soaking the gel in a 2 μg/mL ethidium bromide solution for 15 min at room temperature and then photographed with shortwave UV light to give photograph 1. The ethidium bromide was then rinsed out of the gel by running distilled H_2O over the gel for several hours, and the gel was soaked in 0.01 M $TbCl_3$ and 0.01 M cacodylate (pH 7.0) for 15 min and photographed as above to give photograph 2. The native gel containing native PM2 DNA bands was also first stained with ethidium bromide and photographed as above (photograph 3). The ethidium bromide was again rinsed out and the gel was restained with $TbCl_3$ and photographed (photograph 4). A duplicate sample of native PM2 DNA was electrophoresed on a native gel, which was directly stained with $TbCl_3$ and photographed (photograph 5). 7-s exposures were used for all photographs.

bromide (no. 1, denaturing gel; no. 3, native gel) and then after washing out the ethidium bromide and restaining with $TbCl_3$ (no. 2, denaturing gel; no. 4, native gel); gel no. 5 was a duplicate run of native gel no. 3, but stained only with $TbCl_3$. Not unexpectedly, ethidium bromide shows only an uppermost band in denatured gel no. 1 that must correspond to native material that did not penetrate the gel. By contrast, staining of this gel with $TbCl_3$ (no. 2) reveals a series of single-strand DNA bands of varying size.

Since there are faint bands evident which were visually judged to represent less than 1% of the total fluorescence due to the 6 μg of DNA in slot c of photo no. 2, it would appear that as little as 0.06 μg is readily discernible after $TbCl_3$ staining. An even lower estimate of 0.01 μg of DNA is made upon considering that a region of the smear in slot a in this photo (which contained only 0.5 μg of DNA) corresponding in size to a small band in slot c represents approximately 0.02 of the total smear and should be discernible.

The specificity of $TbCl_3$ stain for single-strand DNA is further seen from a comparison of the staining results with the native gels. Photo no. 3 shows a series of ethidium bromide stained bands. Efforts to wash out this stain and then restain with $TbCl_3$ revealed no new bands and only the one or two uppermost bands observed originally with ethidium bromide (photo no. 4). That no DNA was washed out during the effort to remove the ethidium bromide was shown when the bands seen in photo no. 3 were regained when $TbCl_3$ was removed and the gel restained with ethidium bromide (not shown). Further, since the native gel contained no fluorescent bands after staining directly with $TbCl_3$ (photo no. 5), it is demonstrated that the samples contained no denatured fragments and that the bands seen in photo no. 4 must have been due only to incomplete removal of the ethidium bromide stain. The high degree of specificity of $TbCl_3$ as a stain for only single-strand DNA is therefore confirmed. Thus, $TbCl_3$ provides a highly sensitive complement to ethidium bromide for staining nucleic acids.

Discussion

The conformational specificity of the Tb^{3+} fluorescence enhancement probe obviously has wider applications for nucleic acid investigations than the two described here. The effect has been shown to apply to either DNA or RNA residues. Moreover, measurements can be made quickly and without the need for first separating single- from double-stranded components. The fact that it can be applied on the same sample to identify single-stranded constituents not detectable by ethidium bromide makes the probe particularly useful. It also offers the possibility of detecting transient local melting in nucleic acid helixes or regions of helix defects.

The explanation for the quenching of fluorescence by base-pair formation may lie in the perturbation of the electronic structure of the bases upon hydrogen-bond formation as manifest, for example, by the red shift in the near-ultraviolet CD spectrum (Cantor et al., 1966; Adams et al., 1967). Involvement in base pairing is known to quench the intrinsic fluorescence of m^7G residues (Leng et al., 1968) and of fluorescent derivatives of adenosine (Ward et al., 1969).

In our exploratory studies, the visible fluorescence produced as a consequence of the interaction of the lanthanides, Dy^{3+}, Eu^{3+}, Lu^{3+}, Sm^{3+}, and Tb^{3+}, with the free nucleotides, AMP, GMP, CMP, and UMP, was determined. Only the Tb^{3+} cation exhibited significant fluorescent enhancement as a consequence of the interaction. The reason for this specificity among lanthanides must lie in the fact that Tb has the most appropriate electronic transition to serve as an acceptor for long-distance energy transfer from the near-ultraviolet-absorbing nucleic acid bases. This is because Tb has several low-lying 5d electron levels separated from the next lowest energy level by a gap of appropriate size to generate strong fluorescence in the visible region of the spectrum (Dieke, 1968).

Acknowledgments

We thank Rill Reuter and Michael Goodman for technical assistance and Don McClure, Karen Palter, and Harold Weintraub for helpful suggestions.

References

Adams, A., Lindahl, T., & Fresco, J. R. (1967) *Proc. Natl. Acad. Sci. U.S.A. 57*, 1684–1691.

Barry, C. D., Glasel, J. A., North, A. C. T., Williams, R. J. P., & Xavier, A. V. (1971) *Nature (London) 232*, 236–245.

Britten, R. J., & Kohne, D. R. (1968) *Science (Washington, D.C.) 161*, 529–540.

Cantor, C. R., Jaskunas, S. R., & Tinoco, I., Jr. (1966) *J. Mol. Biol. 20*, 39–62.

Dieke, G. H. (1968) *Spectra and Energy Levels of Rare Earth Ions in Crystals*, p 142, Interscience, New York.

Eichorn, G. L., & Butzow, J. J. (1965) *Biopolymers 3*, 79–94.

Formosa, C. (1973) *Biochem. Biophys. Res. Commun. 53*, 1084–1087.
Fresco, J. R. (1963) in *Informational Macromolecules* (Vogel, H. J., Bryson, V., & Lampen, J. O., Eds.) pp 121–142, Academic Press, New York.
Fresco, J. R., & Massoulie, J. (1963) *J. Am. Chem. Soc. 85*, 1352–1353.
Fresco, J. R., Alberts, B. M., & Doty, P. (1960) *Nature (London) 188*, 98–101.
Grunberg-Manago, M., Ortiz, P. J., & Ochoa, S. (1956) *Biochim. Biophys. Acta 20*, 269–285.
Guschlbauer, W. (1967) *Proc. Natl. Acad. Sci. U.S.A. 57*, 1441–1448.
Guschlbauer, W., Richards, E. G., Beurling, K., Adams, A., & Fresco, J. R. (1965) *Biochemistry 4*, 964–975.
Karpel, R. L., Miller, N. S., Lesk, A. M., & Fresco, J. R. (1975) *J. Mol. Biol. 97*, 519–532.
Karpel, R. L., Bertelsen, A. H., & Fresco, J. R. (1980) *Biochemistry 19*, 504–512.
Leng, M., Pochon, F., & Michelson, A. M. (1968) *Biochim. Biophys. Acta 169*, 350–362.
LePecq, J. B., & Paoletti, C. (1967) *J. Mol. Biol. 27*, 87–106.
Ringer, D. P., Burchett, S., & Kizer, D. E. (1978) *Biochemistry 17*, 4818–4825.
Topal, M., & Fresco, J. R. (1979) *Fed. Proc., Fed. Am. Soc. Exp. Biol. 38*, 501.
Ward, D. C., Reich, E., & Stryer, L. (1969) *J. Biol. Chem. 244*, 1228–1237.
Weintraub, H., & Groudine, M. (1976) *Science (Washington, D.C.) 193*, 848–856.
Weissman, S. I. (1942) *J. Chem. Phys. 10*, 214–217.
Weissman, S. I. (1950) *J. Chem. Phys. 18*, 1258–1262.
Yonuschot, G., & Mushrush, G. W. (1975) *Biochemistry 14*, 1677–1681.
Yuster, P., & Weissman, S. I. (1949) *J. Chem. Phys. 17*, 1182–1188.
Zimmerman, S. B., Cohen, G. H., & Davies, D. R. (1975) *J. Mol. Biol. 92*, 181–192.

Interactions of a New Antitumor Antibiotic BBM-928A with Deoxyribonucleic Acid. Bifunctional Intercalative Binding Studied by Fluorometry and Viscometry†

Cheng-Hsiung Huang,* Seymour Mong, and Stanley T. Crooke

ABSTRACT: A new actinoleukin-like antitumor antibiotic, BBM-928A, has been shown to interact with isolated DNA molecules. BBM-928A contains two substituted quinolines linked by a cyclic decapeptide. Quenching effects of the covalently closed superhelical PM2 DNA on the BBM-928A fluorescence revealed a strong interaction with an apparent association constant of 1.93×10^7 M^{-1} and with 11 deoxyribonucleic acid (DNA) nucleotides per BBM-928A binding site. Viscometric studies indicated that BBM-928A induced an unwinding–rewinding process of the closed superhelical PM2 DNA typically observed for DNA intercalators. The unwinding angle (43°) induced by BBM-928A was almost twice that of the ethidium bromide (26°), a monofunctional intercalator. The BBM-928A-induced increase of the helix length of sonicated rodlike calf thymus DNA was ~1.5-fold that induced by the ethidium bromide. On the basis of these observations, we concluded that BBM-928A bifunctionally intercalated with DNA in a manner similar to the bifunctional intercalation of echinomycin.

A new family of actinoleukin-like antibiotics, BBM-928, has recently been isolated from the fermentation broths of an aerobic strain of actinomycetes. The BBM-928 complex exhibits potent antitumor activity against P388 and L-1210 leukemia, B-16 melanoma, Lewis carcinoma, and sarcoma 180, with a potency about 300–700-fold that of mitomycin C (unpublished data). The biology and chemistry of BBM-928A complex will be published elsewhere.

Figure 1 shows the structure BBM-928A of the BBM-928 complex which contains two substituted quinoline chromophores linked by a cyclic decapeptide. Structurally, the BBM-928 complex is similar to echinomycin (also shown in Figure 1), a quinoxaline antibiotic shown to be capable of bifunctionally intercalating with DNA at low ionic strength (Waring & Wakelin 1974; Wakelin & Waring 1976).

BBM-928, like echinomycin, has a structure with an apparent twofold rotational symmetry (Keller-Schierlein et al., 1959; Sobell et al., 1971) which, if BBM-928 reacts with DNA, would endow the molecule with an ability for bifunctional interactions involving the two chromophores (Wakelin & Waring, 1976).

Data in this report resulted from the first stage of a series of studies designed to understand the mechanism of the antitumor activity of BBM-928. The results indicated that BBM-928A, the most active member of the complex, interacts strongly with isolated DNA molecules through a bifunctional intercalation.

Materials and Methods

Chemicals. BBM-928A and echinomycin were obtained from Bristol Laboratories, Syracuse, NY. Superhelical, covalently closed circular DNA of PM2 bacterial phages (ccc

† From the Bristol-Baylor Laboratory, Department of Pharmacology, Baylor College of Medicine, Texas Medical Center, Houston, Texas 77030 (C.H.H., S.M., and S.T.C.), and the Bristol Laboratories, Syracuse, New York 13201 (S.T.C.). *Received May 12, 1980.* This work was supported in part by a grant from the Bristol Laboratories and by a grant (CA-10893-P12) from the National Cancer Institute.

0006-2960/80/0419-5537$01.00/0